

The Potential of Narrow-Band Imaging as a Novel Light Source for Photodynamic Therapy for Superficial Cancers via Endoscopes

Yusuke Nakada^a, Takaaki Sugihara^{a, c}, Maria Tanaka^a, Wataru Hamamoto^a,
Tsutomu Kanda^a, Takuki Sakaguchi^a, Hiroki Kurumi^a, Takumi Onoyama^a,
Yuichiro Ikebuchi^a, Tomoaki Takata^a, Hajime Isomoto^a,
Naoyuki Yamaguchi^b

Abstract

Background: Photodynamic therapy (PDT) has advanced through the utilization of photosensitizers and specific-wavelength light (≥ 600 nm). However, the widespread adoption of PDT is still impeded by high equipment costs and stringent laser safety requirements. Porphyrins, crucial in PDT, have another absorbance peak of blue light ($\lambda = 380 - 500$ nm). This peak corresponds to the wavelength of narrow-band imaging (NBI) ($\lambda = 390 - 445$ nm), an image-enhancement technology integrated into endoscopes by Olympus Medical Systems. The study aimed to investigate the potential of widely adopted NBI as a PDT light source for superficial cancers via endoscopes.

Methods: Esophageal and biliary cancers were selected for investigation. Human esophageal cancer cell lines (KYSE30, KYSE70, KYSE170) and cholangiocarcinoma cell lines (HuCCT-1, KKKU-213) were subjected to verteporfin-mediated PDT under NBI light ($\lambda = 390 - 445$ nm). Assessments included spectrometry, crystal violet staining, and fluorescein imaging of singlet oxygen generation and apoptosis.

Results: Verteporfin exhibited a peak ($\lambda = 436$ nm) consistent with the NBI spectrum, suggesting compatibility with NBI light. NBI light significantly inhibited the growth of esophageal and biliary cancer cells. The half-maximum effective concentration (EC_{50}) values (5 J/ cm^2) for KYSE30, KYSE70, KYSE170, HuCCT-1, and KKKU-213 were calculated as $2.78 \pm 0.37 \mu M$, $1.76 \pm 1.20 \mu M$, $0.77 \pm 0.16 \mu M$, $0.65 \pm 0.18 \mu M$, and $0.32 \pm 0.04 \mu M$, respectively. Verteporfin ac-

cumulation in mitochondria, coupled with singlet oxygen generation and observed apoptotic changes, suggests effective PDT under NBI light.

Conclusions: NBI is a promising PDT light source for superficial cancers via endoscopes.

Keywords: Cholangiocarcinoma; Esophageal cancer; Endoscope; Narrow-band imaging; Photodynamic therapy; Porphyrins; Verteporfin

Introduction

Over the past century, starting from the 1900s, photodynamic therapy (PDT) has experienced continuous advancements [1]. The procedure involves the administration of a photosensitizer (PS), allowing its accumulation in tissues, followed by exposure to light at a specific wavelength (typically ≥ 600 nm). PDT selectively destroys target tissues by interacting with a PS, specific-wavelength light, and molecular oxygen [2]. This activation produces reactive oxygen species (ROS), including singlet oxygen (1O_2) and radicals. This concept is feasible for cancer treatment. In the 1960s, Lipson et al showed that hematoporphyrin derivative (HPD) localized to tumors [3]; and in 1975, Kelly et al demonstrated that light activation of HPD eliminated bladder carcinoma in mice [4]. These findings opened the new era of PDT. In 1976, the first human PDT trial with HPD was conducted in bladder cancer by Kelly et al [5]. At present, PDT for early-stage lung cancer, superficial esophageal cancer, superficial early gastric cancer, cervical cancer, and dysplasia are covered by insurance in Japan. Distinct from chemotherapy, PDT possesses a unique methodology, suggesting its potential to evolve as a promising medical approach in the future. Although compact and less expensive diode lasers are replacing large and expensive laser systems, the number of facilities where they can be used remains limited. Currently, there are only about 30 facilities in Japan, with the majority being university hospitals. The reasons for this limitation may be attributed to the additional cost (approximately \$57,000) and cost-effectiveness associated with the installation of special-

Manuscript submitted January 2, 2024, accepted February 28, 2024
Published online April 30, 2024

^aDivision of Gastroenterology and Nephrology, Department of Multidisciplinary Internal Medicine, Faculty of Medicine, Tottori University, Yonago 683-8504, Japan

^bDepartment of Endoscopy, Nagasaki University Hospital, Nagasaki 852-85011, Japan

^cCorresponding Author: Takaaki Sugihara, Division of Gastroenterology and Nephrology, Department of Multidisciplinary Internal Medicine, Faculty of Medicine, Tottori University, Yonago 683-8504, Japan.
Email: sugitaka@tottori-u.ac.jp

doi: <https://doi.org/10.14740/gr1694>

ized equipment, the requirement that only individuals who have completed a training program are allowed to use the laser, and the need for safety controls during laser operation, among other barriers to entry.

Therefore, light-emitting diode (LED)-based PDT is currently in development. Our research group has developed an endoscope system for efficient excitation light delivery in photodynamic diagnosis (PDD) or PDT with a simple button interface including LED [6-11]. The creation of a safer method applicable in diverse settings is warranted. In this context, our focus has shifted to more convenient light sources.

Generally, red light with a wavelength of 600 - 800 nm is used in PDT. On the other hand, porphyrins absorb strongly in the 380 - 500 nm range (Soret band) and weakly in the 500 - 750 nm region (Q band) [12]. This indicates that blue light with a wavelength of around 400 nm is advantageous for photoexciting porphyrins. However, blue light, with high absorption by hemoglobin and melanin, penetrates the skin only up to 1 mm [13]. Subsequently, we recognized that this limitation could be overcome by leveraging an endoscope for the direct irradiation of superficial cancers within the body. Additionally, we noticed that specialized lighting for image-enhanced endoscopy (IEE) has recently been integrated into endoscope systems.

IEE is a modality that enhances lesion visibility by intensifying microstructure, blood vessels, and color, resulting in easier detection of gastrointestinal lesions. Among IEE, three technologies are now available for visualizing microvascular imaging using narrow band via endoscopes, narrow-band imaging (NBI) (Olympus Medical Systems, Tokyo, Japan), blue laser imaging (BLI) (Fujifilm Co., Tokyo, Japan), and i-scan OE (PENTAX Medical, Tokyo, Japan) [14]. NBI utilizes the light of two distinct wavelengths: blue: $\lambda = 390 - 445$ nm, and green: $\lambda = 530 - 550$ nm [15, 16]. BLI, on the other hand, employs a narrow-band wavelength at 410 nm [17]. The i-scan OE optical filters enhance overall transmittance by connecting peaks in the hemoglobin absorption spectrum ($\lambda = 415$ nm, 540 nm, and 570 nm) to form a continuous wavelength spectrum [18]. Each of the three companies employs proprietary narrow-wavelength imaging technologies. Given that Olympus dominates 70% of the global market for endoscope systems, utilizing widely adopted endoscope systems using NBI was deemed feasible [19]. Deeper penetration is anticipated by directing the radiation directly to the cancer through the endoscope rather than through the skin. Thus, in this study, we aimed to clarify the potential of NBI as a light source for PDT.

Materials and Methods

Cell lines and cultures

Esophageal and biliary cancer were selected as the primary superficial cancers in our investigation. The human esophageal cancer cell lines KYSE30, KYSE70, and KYSE170 cells were obtained from the JCRB cell bank (Osaka, Japan). The KYSE30 cells were cultured in Dulbecco's modified Eagle

medium (D-MEM) supplemented with 2% fetal bovine serum (FBS). The KYSE70 cells were cultured in D-MEM supplemented with 5% FBS. The KYSE170 cells were cultured in the RPMI-1640/nutrient mixture F-12 medium supplemented with 2% FBS. The human cholangiocarcinoma cell lines HuCCT-1 and KKU-213 cells were obtained from the JCRB cell bank. The HuCCT-1 cells were cultured in RPMI-1640 medium supplemented with 10% FBS. The KKU-213 cells were cultured in the D-MEM supplemented with 10% FBS.

All cell culture media were supplemented with 2 mM L-glutamine solution without antibiotics. The cells were cultured in a humidified incubator with 5% CO₂ at 37 °C.

Reagents

Verteoporphin (VP, SML0534) was purchased from Merck KGaA (Darmstadt, Germany). For cell staining, crystal violet (031-04852) was purchased from Fujifilm Wako Pure Chemical Co., Ltd. (Osaka, Japan). For microscopy, MitoBright Green (MT06) and Hoechst-33342 solution (346-07951) were purchased from Dojindo Laboratories, Co., Ltd. (Kumamoto, Japan). Singlet Oxygen Sensor Green (S36002) was purchased from Thermo Fisher Scientific, Inc. (Tokyo, Japan).

Spectrometry

UV-Vis spectrophotometer (Shimadzu UV-3100PC, Shimadzu Co., Kyoto, Japan) was employed for spectrometry. A linear transmission method was used, taken at a 0-degree injection angle within the 300 - 800 nm wavelength range, utilizing a halogen lamp as the light source and a photomultiplier as the detector. The slit width was set at 5 nm, and the optical path length was 10 mm. Dimethyl sulfoxide (DMSO) served as the reference substance.

PDT protocol

We used the 35-mm dish for culture and crystal violet staining because the NBI irradiation light for VP-PDT is uneven irradiation. The cells were treated with VP in a serum-free medium for 15 min in the dark and then irradiated with NBI light (GIF-HQ290 and EVIS X1 CV-1500; Olympus, Co., Tokyo, Japan) at 2.5 J/cm² for 70 s (35.7 mW/cm²) or 5 J/cm² for 140 s (35.7 mW/cm²). We irradiated the treated cells with NBI light under certain conditions: dark, irradiation distance 18 mm, iris mode average, brightness adjustment +8 (GIF-HQ290 and EVIS X1 CV-1500; Olympus, Co., Tokyo, Japan).

Crystal violet staining

The cells were seeded onto 35-mm dishes. Twenty-four hours after PDT, the cells were fixed with 4% paraformaldehyde for 5 min at 20 - 25 °C, stained with 0.05% crystal violet (CV) for 30 min at 20 - 25 °C, washed with phosphate-buffered saline

(PBS), and dried. Subsequently, methanol was added to dissolve the dye, and the absorbance was measured at 540 nm using a microplate reader (Vientonano; DS Pharma Biochemical Co., Ltd., Osaka, Japan) to evaluate the viability of the cancer cell lines after PDT and the half-maximum effective concentration (EC_{50}) value of VP was calculated.

MTS assay

Cell viability was also assessed using the MTS (3-(4, 5-dimethylthiazol-2-yl)-5-(3-carboxymethoxyphenyl)-2-(4-sulfophenyl)-2H-tetrazolium) assay. The procedure was conducted as follows: 1 mL of culture medium was combined with 200 μ L of CellTiter 96[®] Aqueous One Solution Cell Proliferation Assay (G3580; Promega, Madison, WI). After 1 h of incubation, absorbance was measured at 490 nm using a microplate reader (Viento nano; DS Pharma Biochemical, Osaka, Japan). Cell viability relative to control cells was then calculated.

Microscopic imaging

The cells were visualized using a fluorescence microscope (BZ-X710; Keyence Co., Osaka, Japan). To visualize the VP, a filter cube (OP-87767; Keyence Co., Osaka, Japan) was used with relevant excitation (405BP20) and fluorescence (RPE630LP) filters. To visualize the MitoBright Green and singlet oxygen, the BZ-X filters GFP (OP-87763; Keyence Co., Osaka, Japan) were used. To visualize the Hoechst staining, the BZ-X filters DAPI (OP-87762; Keyence Co., Osaka, Japan) were used. The software BZ-analyzer (Ver.1.3.1.1., Keyence Co., Osaka, Japan) was used to merge, reduce noise, and enhance signal intensity.

Fluorescent staining of intracellular organelles

We observed that VP had a porphyrin structure and emitted red light when the excitation irradiation was 405 nm. Cells were exposed to 0.1 μ M MitoBright Green (10 min, 20 - 25 °C). After washing with PBS twice, cells were incubated with 0.1 μ M VP for 15 min at 37 °C in the dark. This stain accumulates in the mitochondria of live cells based on the mitochondrial membrane potential. After washing with PBS, cells were imaged under a fluorescence microscope (BZ-X710, Keyence Co., Osaka, Japan).

Singlet oxygen staining

The cells were incubated with 2 μ M VP for 15 min at 37 °C in the dark, washed twice with PBS, and exposed to 50 μ M Singlet Oxygen Sensor Green. This reagent emits a green fluorescence signal in the presence of S1 oxygen. NBI light irradiation was performed at 5 J/cm², and after 1 h, the cells were visualized using a fluorescent microscope (BZ-X710, Keyence Co., Osaka, Japan).

Detection of apoptosis

Hoechst staining was performed to detect apoptosis. Cells were incubated with 2 μ M VP for 15 min at 37 °C in the dark. Subsequently, the cells were irradiated with NBI light at 5 J/cm². After NBI light irradiation, the cells were incubated for 12 h at 37 °C, washed, and incubated with 1 μ g/mL Hoechst-33342 solution for 15 min at 20 - 25 °C, avoiding sunlight and room lights. The cells were then visualized using a fluorescence microscope (BZ-X710, Keyence Co., Osaka, Japan).

Statistical analysis

The Dunn test was employed for multiple comparisons, and statistical analyses were conducted using StatFlex software (Windows ver. 6.0; Artech, Osaka, Japan). Statistical significance was defined at $P < 0.05$, and data were presented as mean \pm standard deviation (SD).

Ethical compliance

This study was conducted in compliance with all the applicable institutional ethical guidelines for care and welfare. The Institutional Review Board approval was not applicable.

Results

The Soret peak of VP is consistent with the NBI spectrum

Initially, we analyzed the VP spectrum, observing a prominent absorption peak with a substantial absorption coefficient at 436 nm, known as the Soret peak. Additionally, there were smaller peaks at 579, 629, and 691 nm, forming the Q band (Fig. 1). This indicates that blue light used for NBI with a wavelength of around 436 nm is advantageous for photoexcitation of VP.

NBI light inhibits the growth of both esophageal cancer cells and biliary cancer cells

NBI light was applied to esophageal cancer cells (KYSE-30, KYSE-70, and KYSE-170) and biliary cancer cells (HuCCT-1 and KKU-213). Subsequently, cell growth was assessed via CV staining. KYSE30 and KYSE70 demonstrated significant cell growth inhibition at concentrations of 0.8 μ M (KYSE30: -18.7%, $P < 0.01$; KYSE70: -33.6%, $P < 0.01$) and 3.2 μ M (KYSE30: -47.7%, $P < 0.01$; KYSE70: -63.4%, $P < 0.01$) of VP, respectively, under NBI light irradiation at 5 J/cm² (Fig. 2a, b). Using MTS assay, KYSE30 also demonstrated a similar result at a concentration of 3.2 μ M (-49.7%, $P < 0.05$) of VP under NBI light (5 J/cm²) (Supplementary Material 1, www.gastrores.org). Similarly, KYSE170 exhibited

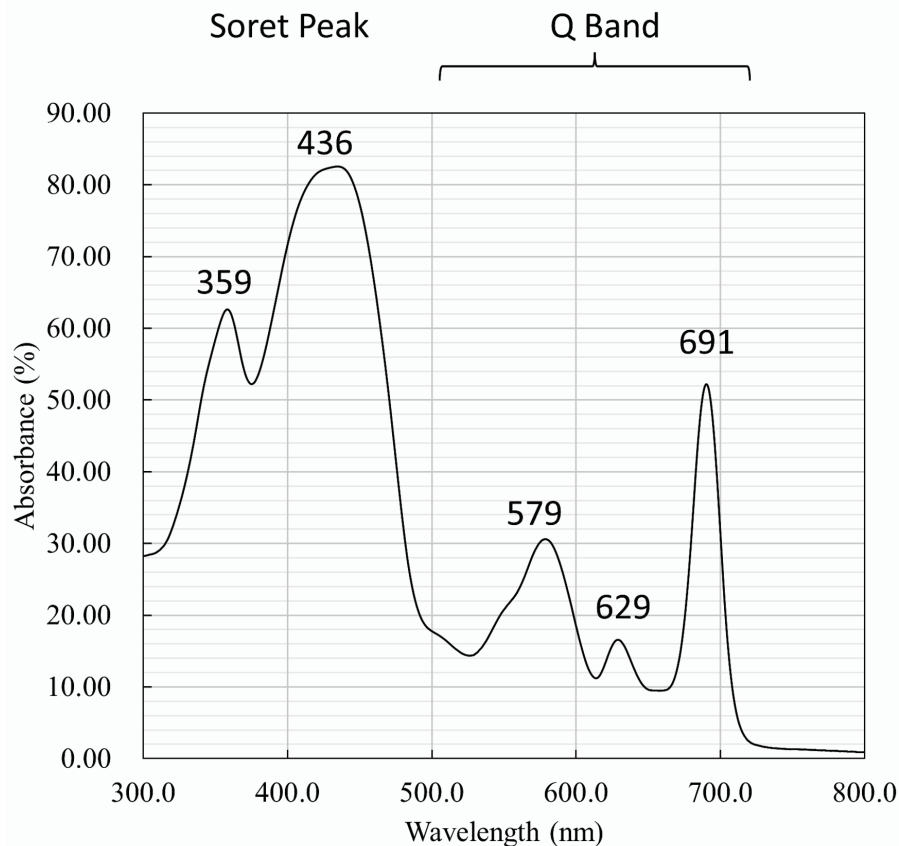


Figure 1. Spectrometry of verteporfin. The spectrum shows a prominent absorption peak at 436 nm, which is known as the Soret peak. Additionally, there are smaller peaks at 579, 629, and 691 nm, which are known as the Q band.

significant suppression at concentrations of 0.4 μM (-32.2%, $P < 0.05$) and 1.6 μM (-59.9%, $P < 0.05$) of VP under 5 J/cm^2 irradiation of NBI light (Fig. 2c). The EC_{50} values (5 J/cm^2) for KYSE30, KYSE70, and KYSE170 were 2.78 ± 0.37 , 1.76 ± 1.20 , and 0.77 ± 0.16 μM , respectively. HuCCT-1 exhibited notable cell growth inhibition at a concentration of 1 μM (-65.8%, $P < 0.01$) of VP under NBI light irradiation at 5 J/cm^2 (Fig. 3a). Similarly, K KU-213 demonstrated significant growth inhibition at a concentration of 0.4 μM (-67.8%, $P < 0.05$) under NBI light irradiation at 5 J/cm^2 (Fig. 3b). The EC_{50} of VP, subsequent to irradiation with 5 J/cm^2 of NBI light, was calculated as 0.65 ± 0.18 μM for HuCCT-1 and 0.32 ± 0.04 μM for K KU-213.

VP accumulation in mitochondria generated singlet oxygen, inducing apoptosis

We further investigated the mechanism of the PDT effect induced by NBI light. VP exhibited accumulation consistent with mitochondria (Fig. 4a). Concurrently, singlet oxygen was generated through NBI light irradiation, consistent with mitochondrial localization (Fig. 4b). Moreover, Hoechst staining demonstrated apoptotic changes in cell nuclei (Fig. 5a-d). These results suggest that NBI light irradiation effectively

serves as a PDT light source.

Discussion

In this study, we have demonstrated that the widely adopted NBI light has the potential to serve as a light source for PDT in the context of superficial cancer via endoscopes. This represents the first report assessing NBI light as a PDT light source.

It has been reported that blue light has various effects on the organism. These effects include both cytoprotective and cytotoxic effects [20]. The cytotoxic effects are related to endogenous photoreceptors. The main photoreceptors are opsins, flavins, porphyrins, and nitrosated proteins [21]. Enzymes that contain porphyrin are present in various cells, such as hemoglobin, cytochrome p-450 enzymes, and the complexes of the electron transport chain [21, 22]. The excitation of intracellular photoreceptors primarily results in the generation of singlet oxygen, which has the potential to interact with nearby molecules, giving rise to additional ROS such as peroxides, superoxide, and hydroxyl radicals. It is reported that irradiation with blue light by excitation of porphyrins leads to ROS formation and demonstrates the toxic effect on microorganisms [21, 23-26]. Our result indicated singlet oxygen was generated by NBI

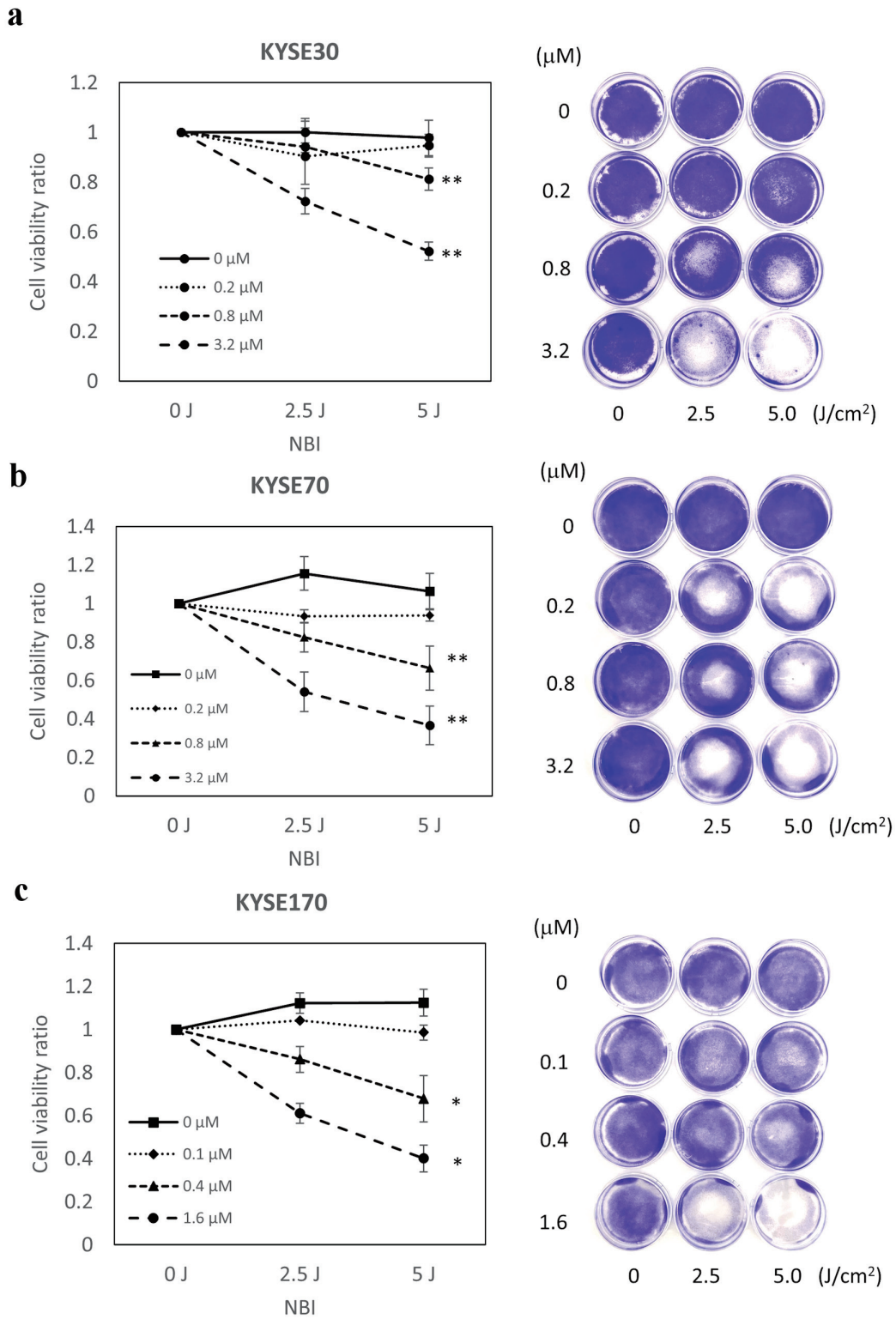


Figure 2. Cell viability assay for esophageal cancer cells. Cell viability was evaluated after staining with crystal violet. (a) KYSE30 and (b) KYSE70 significantly inhibited cell growth at 0.8 μM (KYSE30: -18.7%, $P < 0.01$; KYSE70: -33.6%, $P < 0.01$) and 3.2 μM (KYSE30: -47.7%, $P < 0.01$; KYSE70: -63.4%, $P < 0.01$) concentrations of VP under NBI light (5 J/cm²). (c) KYSE170 also demonstrated significant suppression at 0.4 μM (-32.2%, $P < 0.05$) and 1.6 μM (-59.9%, $P < 0.05$) concentrations of VP under NBI light (5 J/cm²). * $P < 0.05$. ** $P < 0.01$. NBI: narrow-band imaging; VP: verteporfin.

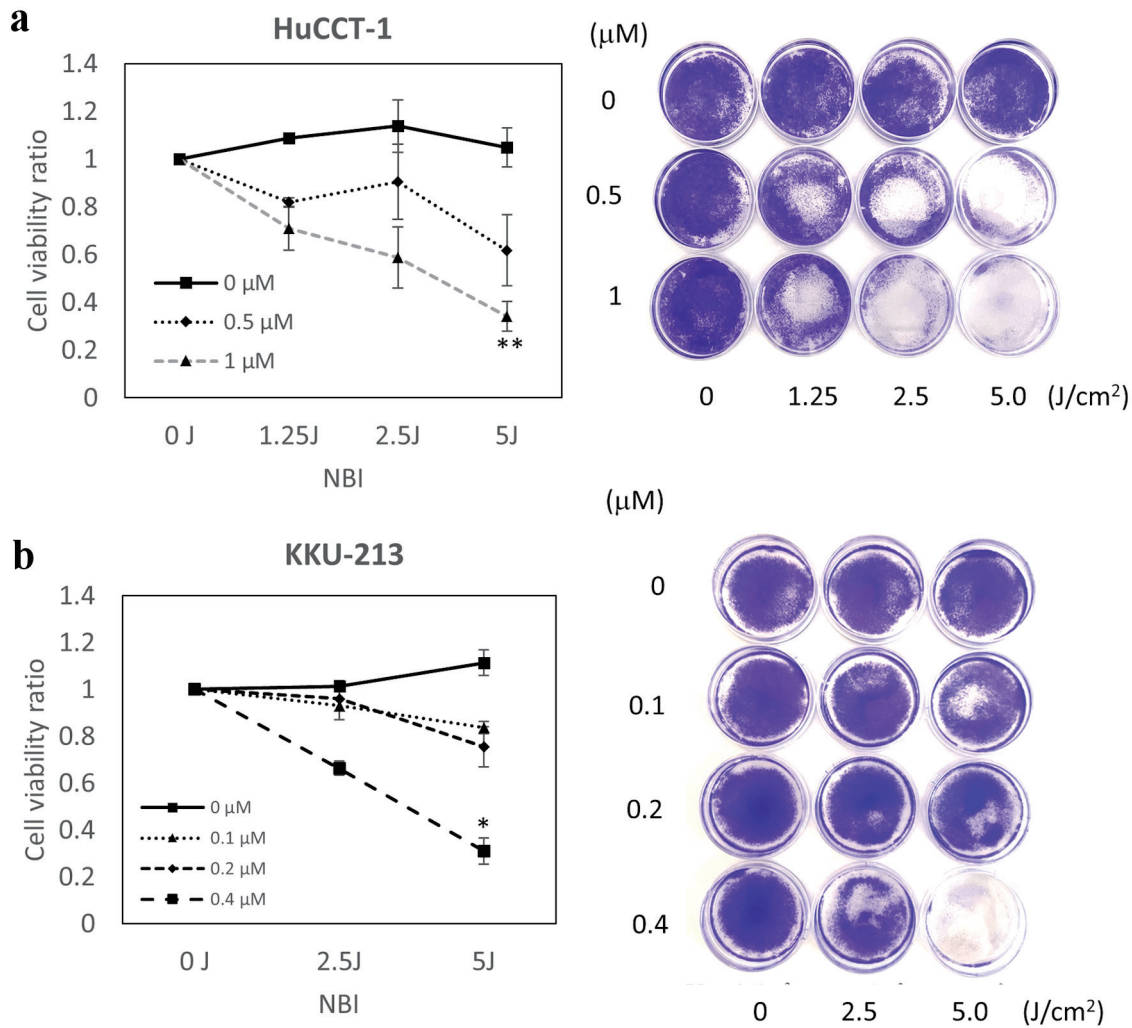


Figure 3. Cell viability assay for biliary cancer cells. Cell viability was evaluated after staining with crystal violet. (a) HuCCT-1 showed marked growth inhibition at 1 μM VP (-65.8%, $P < 0.01$) under NBI light (5 J/cm^2). (b) KKU-213 similarly exhibited significant growth inhibition at 0.4 μM (-67.8%, $P < 0.05$) under NBI light (5 J/cm^2). * $P < 0.05$. ** $P < 0.01$. NBI: narrow-band imaging; VP: verteporfin.

light irradiation. Therefore, NBI light, in combination with VP, is considered to inhibit cancer cell proliferation by ROS production.

Studies suggest that irradiation with blue light inhibits tumor growth in various cancer cell lines through diverse mechanisms [27-34]. In the context of photoreceptors, Ohara et al reported that blue light ($\lambda = 470 \text{ nm}$, irradiance 5.7 mW/cm^2) inhibited the growth of B16 melanoma cells [27]. Furthermore, they also demonstrated that adding riboflavin to the B16 melanoma cells exposed to blue light induced cell damage [35]. Riboflavin, known as vitamin B2, reportedly generates ROS by blue light [36]. In a recent study, Chen et al showed the suppressive effect of blue light ($\lambda = 418 \text{ nm}$ and 457 nm) on the growth of melanoma [37]. The wavelength 457 nm was more effective in inhibiting the growth and migration of B16F10 melanoma cells. Interestingly, Sparsa et al demonstrated clinical efficacy of blue light ($\lambda = 450 \text{ nm}$, 20 J/cm^2 5 days a week

for 2 weeks) without any exogenous PS on an 81-year-old man with malignant melanoma [28]. Zarska et al also evaluated the photodynamic effect of α , β , γ , δ -tetrakis (1-methylpyridinium-4-yl) porphyrin p-toluenesulfonate (TMPyP) and zinc-4-sulfonatophenyl porphyrin (ZnTPPS4) on the HeLa (cervical cancer) and G361 (human skin malignant melanoma) cell lines with blue light ($\lambda = 414 \text{ nm}$) irradiation [32]. Yegorov et al recently reported the toxicity of blue light with porphyrins (cationic porphyrin P4 (TMPyP4) and its amphiphilic derivative porphyrin P1 containing carboxyl groups, as well as their zinc-containing analogues ZnP4 and ZnP1) in normal (human mesenchymal stromal cells KO-16, an immortalized human embryonic fibroblast line (977-hTERT)) and cancer cells (A549 and SK-N-SH) [34]. They demonstrated that in the presence of blue light for 30 min of irradiation, there was a significant decrease in the viability of all cell lines (concentrations 50 nM). The duration of irradiation is far longer than our

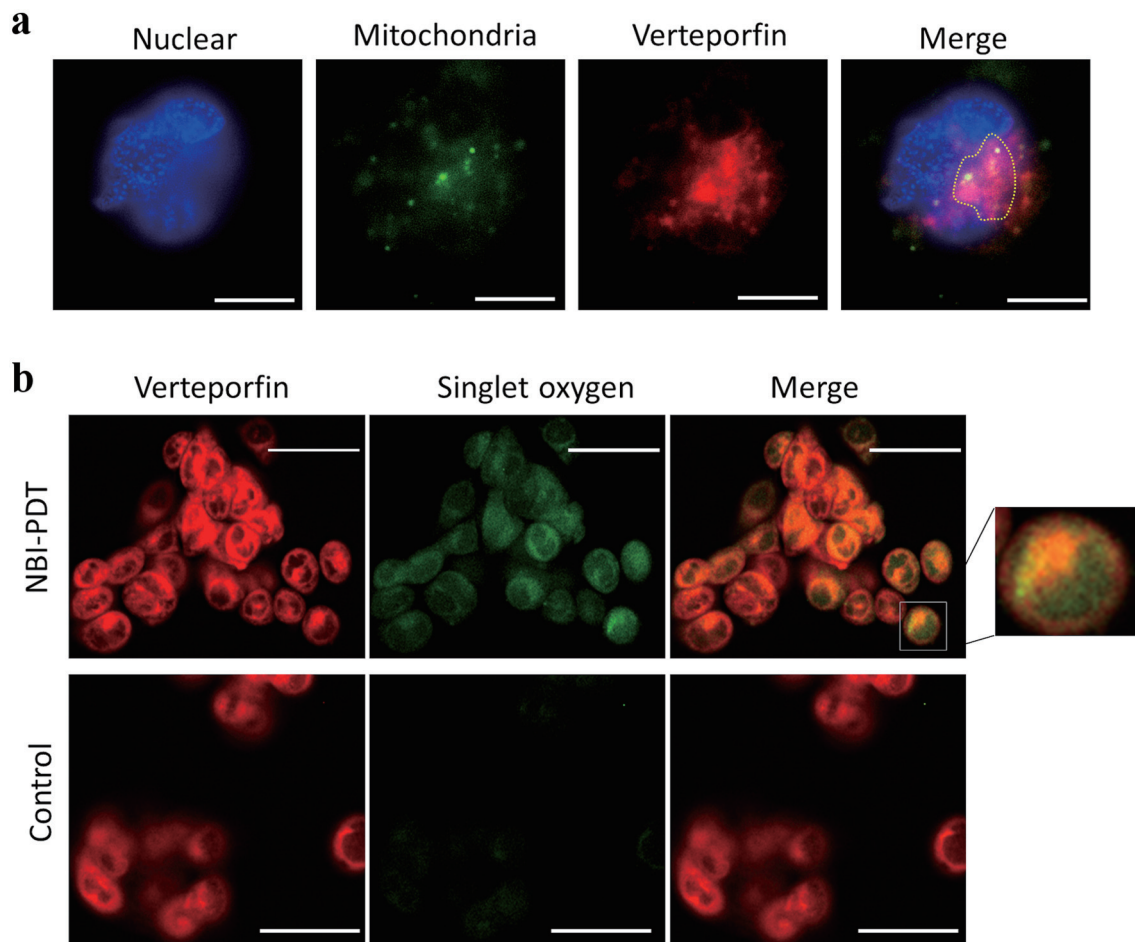


Figure 4. Fluorescein images. (a) Consistency of mitochondria and verteporfin (VP) accumulation. Each image demonstrates nuclear staining, mitochondrial staining (MitoBright Green 0.1 μM for 10 min), VP (0.1 μM for 15 min), and a merged image of mitochondrial staining and VP accumulation. The accumulation of VP consistent with mitochondria is indicated by dotted lines. Original magnification $\times 100$, scale bar = 10 μm . (b) Singlet oxygen induced by NBI-PDT. Each image demonstrates singlet oxygen (Single Oxygen Sensor 50 μM for 60 min), VP, and a merged image of singlet oxygen and VP for both the NBI-PDT and control groups. Singlet oxygen was induced only by NBI-PDT. The accumulation of VP is consistent with singlet oxygen. NBI was irradiated at 5 J/cm^2 (original magnification $\times 40$, scale bar = 50 μm). NBI: narrow-band imaging; PDT: photodynamic therapy.

study, and it suggests that longer irradiation may be toxic to normal cells.

According to the reports, wavelengths of between 414 - 470 nm were used for irradiation on cancer cells. The Soret peak of VP was 436 nm; therefore, if using VP as an exogenous PS, NBI is feasible for the light source.

Endoscopic submucosal dissection (ESD) is commonly employed in managing superficial esophageal cancer, typically when the invasion is limited to the mucosal or submucosal layer. In Japan, conventional PDT has been approved as an alternative to ESD for early-stage esophageal cancer localized within the intraepithelial and mucosal layers, as well as for recurrent esophageal cancer following radiotherapy or chemoradiotherapy. This suggests that NBI-PDT can serve the same population as conventional PDT. Additionally, it may also provide palliative irradiation for cases of malignant obstruction [38]. On the other hand, in unresectable cholangiocarcinoma, PDT is the only evidence-based endoscopic local therapy other

than stenting that enhances the quality of life in bile duct cancer patients [39]. For the biliary tract, the CHF TYPE B260, an ultrafine-diameter Olympus electron scope, can be used with NBI.

The widespread adoption of a light source is crucial for extending the benefits of PDT to a large patient population. As demonstrated in this study, the prevalence of light sources of NBI, already integrated into numerous instruments, signifies the accessibility of endoscopic blue light with anticancer properties. We anticipate the integration of PDT mode into NBI in the future.

This study has a few limitations. Firstly, we did not assess the depth effect of NBI since we only used a two-dimensional (2D) culture. Nevertheless, we have concluded that, for the current study's aim of determining whether NBI can be used for PDT, 2D cultures are adequate. Additionally, we did not conduct an *in vivo* evaluation. This is because the subcutaneous transplantation model in mice, commonly used for evalu-

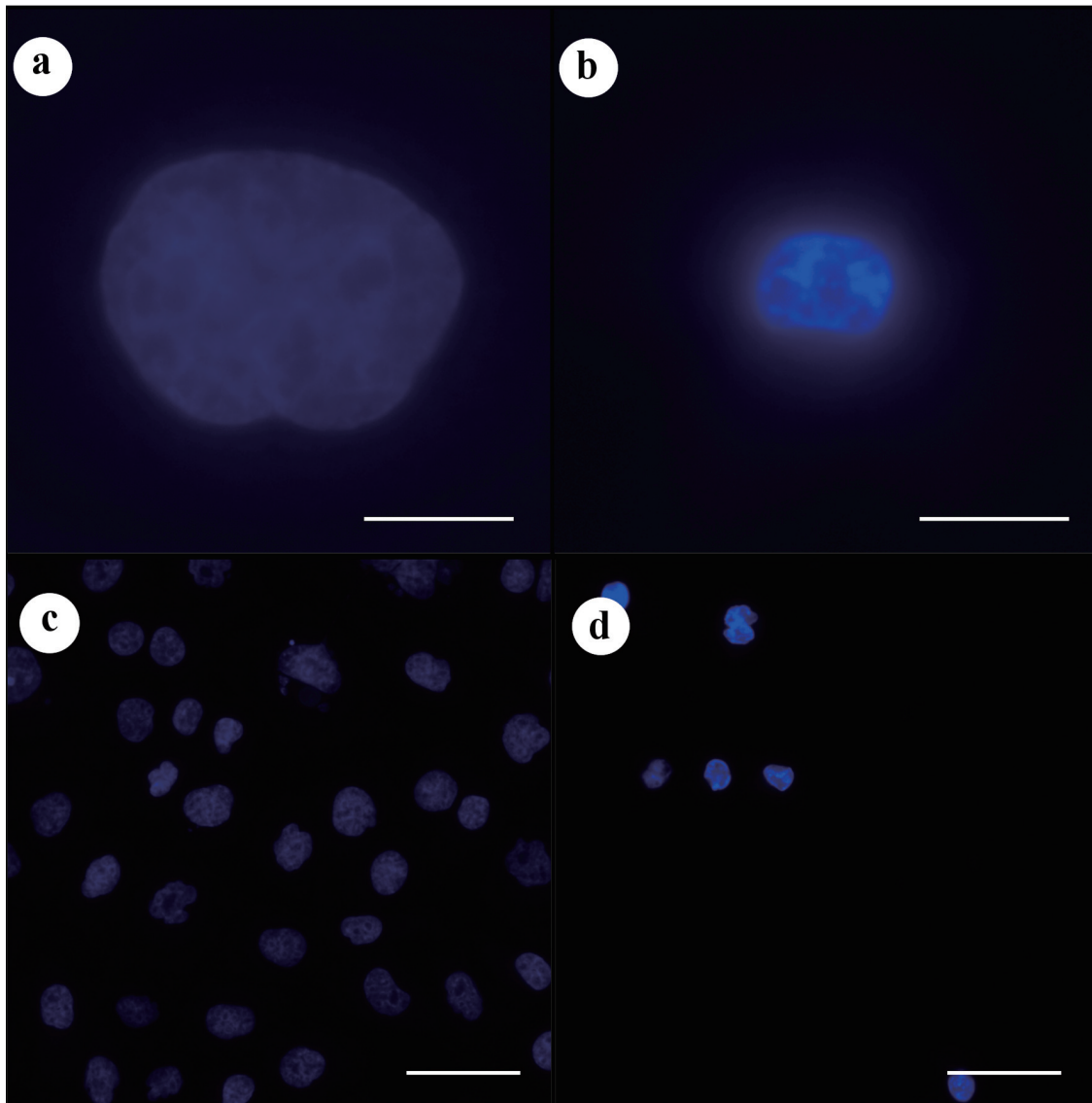


Figure 5. Hoechst staining assessing apoptosis. (a) Control. (b) NBI-PDT. (c) Control. (d) NBI-PDT. Hoechst staining revealed apoptotic changes in cell nuclei under NBI light (5 J/cm^2). Original magnification $\times 100$ with a scale bar of $10 \mu\text{m}$ for (a) and (b), and original magnification $\times 20$ with a scale bar of $50 \mu\text{m}$ for (c) and (d). NBI: narrow-band imaging; PDT: photodynamic therapy.

ation, is hindered by the influence of the epidermal layer on NBI irradiation sites, limiting accurate assessment of tumor suppression. Future studies should consider assessing NBI effects in models allowing direct evaluation of irradiation effects, such as the peritoneal seeding model. Furthermore, it remains to be demonstrated whether NBI affects non-tumorous regions, particularly surrounding areas, in daily practice. For future application in humans, we consider that utilizing a porcine model is the optimal approach to assess the effects on normal tissues. Specifically, after intravenous administration of the same dose of VP in the porcine model as in humans, NBI is applied to the esophageal mucosa and bile duct epithelium using an endoscope, and normal tissue damage is assessed through pathological analysis. Despite these limitations, the study successfully achieved its objective by showcasing the

promising potential of the widely available NBI light source for PDT applications.

In conclusion, our study could demonstrate that the NBI light source has the potential to serve as a light source for PDT in the context of superficial cancer via endoscopes.

Supplementary Material

Suppl 1. Cell viability assessment with MTS assay.

Acknowledgments

None to declare.

Financial Disclosure

All authors have nothing to declare.

Conflict of Interest

All authors have nothing to declare.

Informed Consent

Not applicable.

Author Contributions

YN, TS (Takaaki Sugihara), and TK conceived and planned the experiments. YN, TS (Takaaki Sugihara), MT, WH, TO, and TK conducted the experiments. TS (Takuki Sakaguchi), HK, YI, and TT contributed to interpreting the results. YN and TS (Takaaki Sugihara) wrote the manuscript, and NY and HI supervised the project. All authors provided critical feedback and helped shape the research, analysis, and manuscript.

Data Availability

The datasets used and analyzed in this study are available from the corresponding author upon reasonable request.

Abbreviations

IEE: image-enhanced endoscopy; HOD: hematoporphyrin derivative; NBI: narrow-band imaging; PDD: photodynamic diagnosis; PDT: photodynamic therapy; PS: photosensitizer; ROS: reactive oxygen species; VP: verteporfin

References

- Dolmans DE, Fukumura D, Jain RK. Photodynamic therapy for cancer. *Nat Rev Cancer*. 2003;3(5):380-387. [doi](#) [pubmed](#)
- Correia JH, Rodrigues JA, Pimenta S, Dong T, Yang Z. Photodynamic therapy review: principles, photosensitizers, applications, and future directions. *Pharmaceutics*. 2021;13(9):1332. [doi](#) [pubmed](#) [pmc](#)
- Lipson R, Baldes E, Olsen A. The use of a derivative of hematoporphyrin in tumor detection. *Subject Strain Bibliography*. 1961;26:1-11.
- Kelly JF, Snell ME, Berenbaum MC. Photodynamic destruction of human bladder carcinoma. *Br J Cancer*. 1975;31(2):237-244. [doi](#) [pubmed](#) [pmc](#)
- Kelly JF, Snell ME. Hematoporphyrin derivative: a possible aid in the diagnosis and therapy of carcinoma of the bladder. *J Urol*. 1976;115(2):150-151. [doi](#) [pubmed](#)
- Ogihara K, Isomoto H, Kurumi H, Kanda T, Hashisako M, Tabata K, Ishii H, et al. Expression of coproporphyrinogen oxidase is associated with detection of upper gastrointestinal carcinomas by 5-aminolevulinic acid-mediated photodynamic diagnosis. *Photodiagnosis Photodyn Ther*. 2017;19:15-21. [doi](#) [pubmed](#)
- Kurumi H, Kanda T, Kawaguchi K, Yashima K, Koda H, Ogihara K, Matsushima K, et al. Protoporphyrinogen oxidase is involved in the fluorescence intensity of 5-aminolevulinic acid-mediated laser-based photodynamic endoscopic diagnosis for early gastric cancer. *Photodiagnosis Photodyn Ther*. 2018;22:79-85. [doi](#) [pubmed](#)
- Sakaguchi T, Kinoshita H, Ikebuchi Y, Kanda T, Yamashita T, Kurumi H, Fujii M, et al. Next-generation laser-based photodynamic endoscopic diagnosis using 5-aminolevulinic acid for early gastric adenocarcinoma and gastric adenoma. *Ann Gastroenterol*. 2020;33(3):257-264. [doi](#) [pubmed](#) [pmc](#)
- Mae Y, Kanda T, Sugihara T, Takata T, Kinoshita H, Sakaguchi T, Hasegawa T, et al. Verteporfin-photodynamic therapy is effective on gastric cancer cells. *Mol Clin Oncol*. 2020;13(3):10. [doi](#) [pubmed](#) [pmc](#)
- Kurumi H, Kanda T, Ikebuchi Y, Yoshida A, Kawaguchi K, Yashima K, Isomoto H. Current status of photodynamic diagnosis for gastric tumors. *Diagnostics (Basel)*. 2021;11(11):1967. [doi](#) [pubmed](#) [pmc](#)
- Edano M, Kanda T, Tarumoto R, Hamamoto W, Hasegawa T, Mae Y, Onoyama T, et al. Intracellular glutathione levels affect the outcomes of verteporfin-mediated photodynamic therapy in esophageal cancer cells. *Photodiagnosis Photodyn Ther*. 2022;40:103090. [doi](#) [pubmed](#)
- Giovannetti R, Uddin J. The use of spectrophotometry UV-Vis for the study of porphyrins. *Macro To Nano Spectroscopy*. 2012. [doi](#)
- Ash C, Dubec M, Donne K, Bashford T. Effect of wavelength and beam width on penetration in light-tissue interaction using computational methods. *Lasers Med Sci*. 2017;32(8):1909-1918. [doi](#) [pubmed](#) [pmc](#)
- Nagai M, Suzuki S, Minato Y, Ishibashi F, Mochida K, Ohata K, Morishita T. Detecting colorectal lesions with image-enhanced endoscopy: an updated review from clinical trials. *Clin Endosc*. 2023;56(5):553-562. [doi](#) [pubmed](#) [pmc](#)
- Sano Y, Kobayashi M, Kozu T. Development and clinical application of a narrow band imaging (NBI) system with built-in narrow-band RGB filters. *Stomach and Intestine*. 2001;36:1283-1287. (in Japanese)
- Sano Y. NBI story. *Early Colorectal Cancer*. 2007; 11:91-92. (in Japanese)
- Morimoto Y, Kubo M, Kuramoto M, Yamaguchi H, Kaku T. Development of a new generation endoscope system with lasers "LASEREO." *Fujifilm Research & Development*. 2013;58:1-6.
- i-scan OE Technology. <https://i-scanimaging.com/emea/about/i-scan-oe/i-scan-oe-technology/>. Accessed Dec 30, 2023.
- Fiscal Year Ended Mar 31, 2019. Integrated Report: OLYMPUS. <https://www.olympus-global.com/ir/data/in->

- tegratedreport/2019.html?page=ir. Accessed Dec 30, 2023.
20. Sadowska M, Narbutt J, Lesiak A. Blue light in dermatology. *Life (Basel)*. 2021;11(7):670. [doi](#) [pubmed](#) [pmc](#)
 21. Garza ZCF, Born M, Hilbers PAJ, van Riel NAW, Liebmann J. Visible blue light therapy: molecular mechanisms and therapeutic opportunities. *Curr Med Chem*. 2018;25(40):5564-5577. [doi](#) [pubmed](#)
 22. Serrage H, Heiskanen V, Palin WM, Cooper PR, Milward MR, Hadis M, Hamblin MR. Under the spotlight: mechanisms of photobiomodulation concentrating on blue and green light. *Photochem Photobiol Sci*. 2019;18(8):1877-1909. [doi](#) [pubmed](#) [pmc](#)
 23. Maclean M, McKenzie K, Anderson JG, Gettinby G, MacGregor SJ. 405 nm light technology for the inactivation of pathogens and its potential role for environmental disinfection and infection control. *J Hosp Infect*. 2014;88(1):1-11. [doi](#) [pubmed](#)
 24. Maclean M, Macgregor SJ, Anderson JG, Woolsey GA. The role of oxygen in the visible-light inactivation of *Staphylococcus aureus*. *J Photochem Photobiol B*. 2008;92(3):180-184. [doi](#) [pubmed](#)
 25. Dai T, Gupta A, Murray CK, Vrahas MS, Tegos GP, Hamblin MR. Blue light for infectious diseases: *Propionibacterium acnes*, *Helicobacter pylori*, and beyond? *Drug Resist Updat*. 2012;15(4):223-236. [doi](#) [pubmed](#) [pmc](#)
 26. Hamblin MR, Viveiros J, Yang C, Ahmadi A, Ganz RA, Tolkoff MJ. *Helicobacter pylori* accumulates photoactive porphyrins and is killed by visible light. *Antimicrob Agents Chemother*. 2005;49(7):2822-2827. [doi](#) [pubmed](#) [pmc](#)
 27. Ohara M, Kawashima Y, Katoh O, Watanabe H. Blue light inhibits the growth of B16 melanoma cells. *Jpn J Cancer Res*. 2002;93(5):551-558. [doi](#) [pubmed](#) [pmc](#)
 28. Sparsa A, Faucher K, Sol V, Durox H, Boulinguez S, Doffoel-Hantz V, Calliste CA, et al. Blue light is phototoxic for B16F10 murine melanoma and bovine endothelial cell lines by direct cytotoxic effect. *Anticancer Res*. 2010;30(1):143-147. [pubmed](#)
 29. Oh PS, Na KS, Hwang H, Jeong HS, Lim S, Sohn MH, Jeong HJ. Effect of blue light emitting diodes on melanoma cells: involvement of apoptotic signaling. *J Photochem Photobiol B*. 2015;142:197-203. [doi](#) [pubmed](#)
 30. Del Olmo-Aguado S, Nunez-Alvarez C, Osborne NN. Blue light action on mitochondria leads to cell death by necroptosis. *Neurochem Res*. 2016;41(9):2324-2335. [doi](#) [pubmed](#)
 31. Oh PS, Hwang H, Jeong HS, Kwon J, Kim HS, Kim M, Lim S, et al. Blue light emitting diode induces apoptosis in lymphoid cells by stimulating autophagy. *Int J Biochem Cell Biol*. 2016;70:13-22. [doi](#) [pubmed](#)
 32. Zarska L, Mala Z, Langova K, Malina L, Binder S, Bajgar R, Kolarova H. The effect of two porphyrine photosensitizers TMPyP and ZnTPPS(4) for application in photodynamic therapy of cancer cells in vitro. *Photodiagnosis Photodyn Ther*. 2021;34:102224. [doi](#) [pubmed](#)
 33. Yoshimoto T, Shimada M, Tokunaga T, Nakao T, Nishi M, Takasu C, Kashiwara H, et al. Blue light irradiation inhibits the growth of colon cancer and activation of cancer-associated fibroblasts. *Oncol Rep*. 2022;47(5):104. [doi](#) [pubmed](#) [pmc](#)
 34. Yegorov YE, Vishnyakova KS, Pan X, Egorov AE, Popov KV, Tevonyan LL, Chashchina GV, et al. Mechanisms of phototoxic effects of cationic porphyrins on human cells in vitro. *Molecules*. 2023;28(3):1090. [doi](#) [pubmed](#) [pmc](#)
 35. Ohara M, Fujikura T, Fujiwara H. Augmentation of the inhibitory effect of blue light on the growth of B16 melanoma cells by riboflavin. *Int J Oncol*. 2003;22(6):1291-1295. [pubmed](#)
 36. Liang JY, Yuann JM, Cheng CW, Jian HL, Lin CC, Chen LY. Blue light induced free radicals from riboflavin on *E. coli* DNA damage. *J Photochem Photobiol B*. 2013;119:60-64. [doi](#) [pubmed](#)
 37. Chen Z, Li W, Hu X, Liu M. Irradiance plays a significant role in photobiomodulation of B16F10 melanoma cells by increasing reactive oxygen species and inhibiting mitochondrial function. *Biomed Opt Express*. 2020;11(1):27-39. [doi](#) [pubmed](#) [pmc](#)
 38. Bartusik-Aebischer D, Osuchowski M, Adamczyk M, Stopa J, Cieslar G, Kawczyk-Krupka A, Aebischer D. Advancements in photodynamic therapy of esophageal cancer. *Front Oncol*. 2022;12:1024576. [doi](#) [pubmed](#) [pmc](#)
 39. Cheon YK. Recent advances of photodynamic therapy for biliary tract cancer. *International Journal of Gastrointestinal Intervention*. 2021;10(3):96-100.